Journal of Power Sources 217 (2012) 303–308

Contents lists available at SciVerse ScienceDirect

Journal of Power Sources

journal homepage: www.elsevier.com/locate/jpowsour

Sn nanoparticles grown on graphene for enhanced electrochemical properties

Z. Qin [a], Z.J. Li [b,*], M. Zhang [b], B.C. Yang [b,*], R.A. Outlaw [c]

[a] College of Mathematics and Information Science, North China University of Water Resources and Electric Power, Zhengzhou 450011, China
[b] Institute of Nano Functional Materials, Huanghe University of Science & Technology, Zhengzhou 450006, China
[c] Department of Applied Science, College of William and Mary, Williamsburg, VA 23185, USA

HIGHLIGHTS

- Sn nanoparticles grew on the surface of graphene sheets directly.
- Sn nanoparticles act as a spacer to effectively separate graphene sheets.
- Sn–Gr nanocomposite have much better electrochemical properties than that of pristine graphene.

ARTICLE INFO

Article history:
Received 17 January 2012
Received in revised form
3 June 2012
Accepted 6 June 2012
Available online 19 June 2012

Keywords:
Graphene
Tin nanoparticles
Carbon materials
Supercapacitor

ABSTRACT

Sn nanoparticle decorated graphene (Sn–Gr) materials were prepared by adding tin powder to the reaction of graphite oxide during thermal reduction. In this reaction, Sn nanoparticles were directly grown on the surface of graphene sheets. The Sn nanoparticles were distributed on the surface of Gr sheets uniformly, in which Sn nanoparticles act as a spacer to effectively separate graphene sheets. Sn–Gr electrodes exhibit a high specific capacitance of ~320 F g^{-1} at scan rate of 10 mV s^{-1} in 2 M KNO_3 aqueous solution. The high specific capacitance and charge/discharge rates offered by such hybrid structures make them promising candidates as electrodes in supercapacitors with both high energy and power density.

1. Introduction

Supercapacitors have attracted much attention as novel energy storage devices because of their high power density, long cycling life, and short charging time [1,2], which can be applied to a large variety of applications, including portable electronics, memory backup systems, hybrid electric vehicles, and industrial scale power and energy management [3–6]. There are two energy storage mechanisms for supercapacitors: pseudocapacitance and electrochemical double-layer capacitance (EDLC). Metal oxides such as RuO_2, MnO_2, MoO_3, SnO_2, and electronically conducting polymers [7–9], or their composites, have been used to increase specific capacitance via pseudocapacitive redox reactions. In EDLC, the capacitance comes from the charge accumulated at the electrode–electrolyte interface. Various carbon-based materials such as activated carbon (AC), carbon nanotubes (CNTs), and other carbon materials have been investigated for use as the electrodes in EDL capacitors [5,10–12]. Activated carbon has long been used in commercial supercapacitors because of its high specific capacitance and low cost. This material is still the most popular supercapacitor electrode material to date. However, the specific capacitance of AC decreases dramatically with increased charging/discharging rate. CNTs, especially single-walled CNTs (SWNTs), with a high conductivity and regular porous structure have also been explored as supercapacitor electrode materials. However, the high cost for preparation of high-quality SWNTs restricts their large-scale application in supercapacitors.

As a new carbonaceous materials, graphene (Gr) with maximum surface area of 2630 m^2 g^{-1} and high intrinsic electrical conductivity is believed to be a type of potential energy storage material for EDLC applications [13,14]. A specific capacitance of 100–205 F g^{-1} has been obtained in a KOH aqueous solution, and 156.5 F g^{-1} in a H_2SO_4 aqueous solution. In ionic liquids, the specific capacitance of Gr reached 166 F g^{-1} [15]. However, the restacking of

* Corresponding authors. Tel./fax: +86 371 87541018.
E-mail addresses: ZijiongL@gmail.com (Z.J. Li), Shimoxi2011@126.com (B.C. Yang).

0378-7753/$ – see front matter © 2012 Elsevier B.V. All rights reserved.
http://dx.doi.org/10.1016/j.jpowsour.2012.06.028

Gr sheets during its processing as a result of the strong sheet-to-sheet van der Waals interactions limits its capacitance and practical applications. Up to now, to avoid restacking of Gr nanosheets and obtain Gr with a high available effective surface area is still a challenging question. In order to reduce the restacking of the Gr sheets and obtain the Gr with good electrical conductivity, some inorganic nanoparticles, such as metals or semiconductors have been intercalated into the Gr nanosheets [16,17]. Supporting other electrochemically active materials uniformly on the surface of Gr sheets offers an effective method to minimize aggregation and maximize the accessible area to the electrolyte [18]. Past research has shown that Gr–CNT composites also exhibit a specific capacitance value as high as 320 F g^{-1} [19]. The role of CNTs as a spacer avoids the aggregation of Gr during the reduction. On the other hand, Sn and Sn based compounds have also been reported as high capacity spacers for anode materials [20].

Here, we report a simple way to synthesize Sn nanoparticle decorated graphene (Sn–Gr) materials. This strategy provides a novel method for the preparation of highly active materials (Sn nanoparticles) directly grown on the Gr surface which avoids the restacking of Gr sheets. The resulting structure exhibits a high specific capacitance.

2. Experimental

2.1. Synthesis of GO

Graphite oxide (GO) was prepared from natural graphite powder by the modified Hummers method [22]. Graphite powder (0.5 g), sodium nitrate (0.55 g) and sulfuric acid (23 ml) were mixed and stirred for 10 min. Then, potassium permanganate (3 g) was added slowly with the temperature maintained below 20 °C. Deionized (DI) water was added slowly and the temperature of the solution was raised to 90 °C. The solution turned bright yellow when 3 ml of hydrogen peroxide (30%) was added. The mixture was filtered while warm and washed with warm DI water. The GO was subjected to dialysis to completely remove metal ions and acids. Finally, the product was dried in air at room temperature.

2.2. Synthesis of Sn–Gr nanocomposites

The synthesis of Sn–Gr composites was carried out in a horizontal tube furnace. 50 mg of Sn metal powder was placed at the center of the tube. The GO (0.1 g) was placed in a downstream position from the tin material. After the tube was evacuated to a base pressure of $\sim 1 \times 10^{-3}$ Torr, the Sn and GO materials were heated to1000 °C at a rate of 20 °C min^{-1}, and then maintained at this temperature for 2 h. During the growth process, a carrier gas of argon premixed with 5% hydrogen was fed at a total flow rate of 20 sccm.

2.3. Characterization

The microstructure of the samples was investigated by a SEM (Quanta FEG 250) and TEM (JEOL JEM2010). Raman spectroscopic characterization was recorded on a Horiba Jobin-Yvon LabRam instrument at a laser excitation wavelength of 514 nm. For TEM investigations, the samples were sprayed onto carbon coated copper grids.

2.4. Fabrication of supercapacitor electrodes and electrochemical measurements

The working electrode was prepared as follows: ~1 mg of as-synthesized material was first mixed with polytetrafluoroethylene (60 wt.% water suspension, Aldrich) in a ratio of 100:1 by weight, and then dispersed in ethanol. The suspension was drop-dried into a 1 cm × 1 cm Ni foam (2 mm thick) at 80 °C. The loaded foam was compressed before measurement.

The electrochemical measurements, including cyclic voltammograms (CVs), galvanostatic charge/discharge, and electrochemical impedance spectroscopy were performed in a three-electrode setup: a Ni foam coated with the active materials served as the working electrode. A platinum foil electrode, and a saturated calomel electrode (SCE) served as the counter and reference electrodes, respectively. The electrochemical measurements were carried out on a RST 5202 electrochemical workstation in a 2 M KNO_3 aqueous electrolyte at room temperature.

3. Results and discussion

A field-emission SEM was used to examine the morphology of the as-synthesized samples. Fig. 1(a) is a high magnification SEM image of the Gr sheets after the GO materials were reduced without Sn metal. It is clearly seen that the Gr nanosheets are almost completely transparent and crumpled to a curly, wavy shape. The edges of the sheets are partially folded so that the total surface energy should be reduced. Due to the corrugated nature of the Gr sheets, substantial voids exist between individual Gr sheets. Fig. 1(b) and (c) are the typical SEM images of the Sn–Gr composite. The Sn particles, with average diameter of 20 nm, are near uniformly distributed over the surface of the Gr sheets. The energy dispersive spectrum (EDS) of this region confirms the presence of C, Sn and O (as shown in Fig. 1(d)) and reveals that the structures consists of C, Sn, and O elements. The atomic ratio of C, Sn, and O is approximately 4.5:1:2.

The morphology of the Sn–Gr materials was further analyzed by TEM. Fig. 2a is a typical low-resolution TEM image of Sn–Gr. Sn nanoparticles are uniformly distributed on Gr sheet substrate. Fig. 2b is the high-resolution TEM (HRTEM) image of Sn–Gr materials. The inset in Fig. 2b is a lattice image of Sn nanoparticles, in which the Sn structure can be identified with the clear interplanar distance of 0.291 nm [21].

Fig. 3a shows an X-ray diffraction (XRD) pattern of the as-synthesized Sn–Gr composite. The major diffraction peaks are from C, Sn. The characteristic diffraction peaks with high intensity correspond to the metallic Sn nanoparticles. The (002) plane peak of graphite is broad and its intensity is weak, which indicates that the Sn nanoparticles are distributed evenly on the surface of Gr. The crystalline structure of Gr–Sn composites were further investigated by means of Raman spectroscopy (Fig. 3b). The broad peaks at 1355 cm^{-1} and 1605 cm^{-1}, which are assigned to the D and G peaks of the graphite. Compared with Gr, the broadening of D bands in Gr–Sn sample indicates the decrease of the size of the in-plane sp^2 domains [3]. No other Raman peak appeared in the spectrum, indicating Sn nanoparticles were not oxidized because SnO_2 usually shows strong Raman spectra [22]. TGA analysis of Sn–Gr composite was performed to find out metal content in the sample. Fig. 3c shows the TGA profiles of Sn–Gr composite measured in air conditions. The residual weight percentage was about 39%. As the residues were metal oxides, the metal content of each sample was calculated to be ~23%. In addition, the lower thermal stability of the Sn–Gr compared to the pristine graphene may be due to the catalytic decomposition of Sn oxide since carbon has been reported to catalytically decompose oxides such as RuO_2. Fig. 3d presents the N_2 adsorption/desorption isotherms of Sn–Gr composite. N_2 adsorption/desorption isotherms were obtained by a gas adsorption analyzer at 77 K. The specific surface area was calculated from the Brunauer–Emmett–Teller (BET) plot of the nitrogen adsorption isotherm. By comparison, the specific surface area of the Sn–Gr

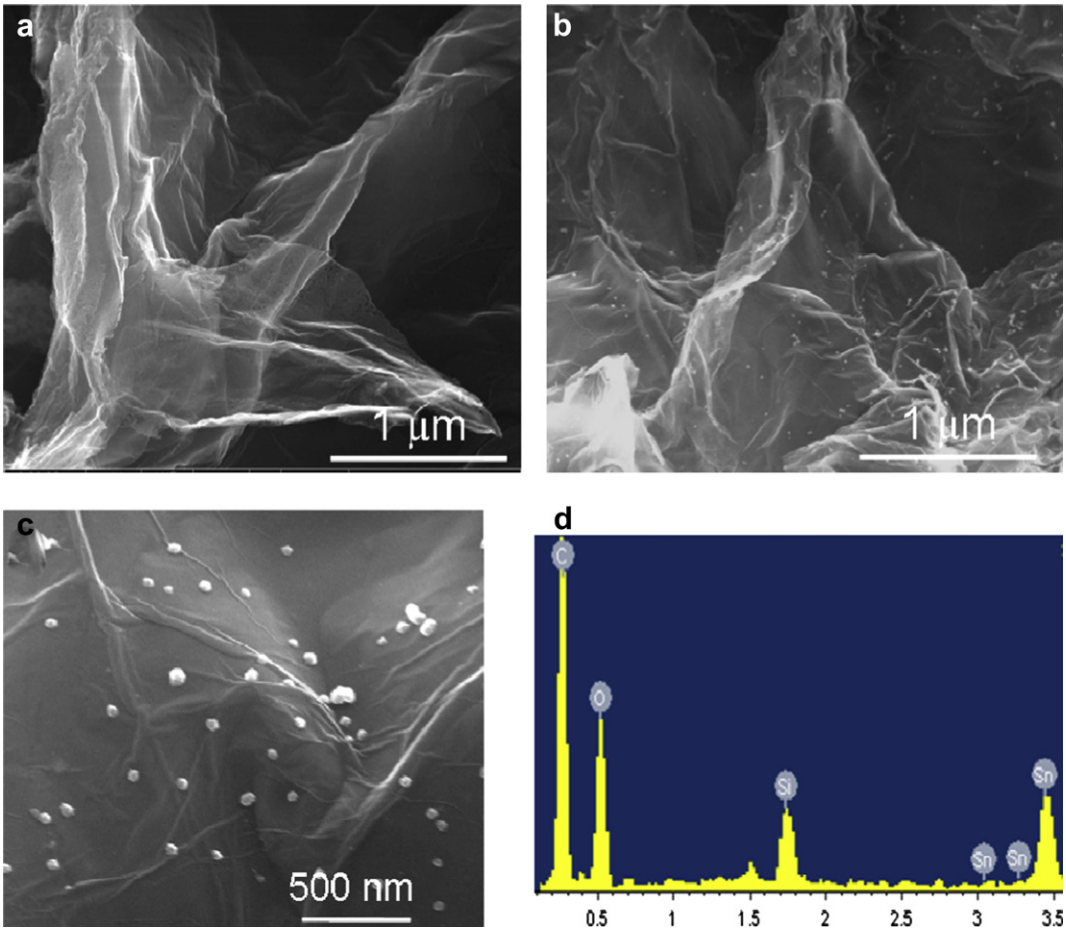

Fig. 1. (a) Typical SEM images of graphene oxide, (b) low magnification and (c) high magnification SEM image of Sn–Gr nanocomposites, EDS of Sn–Gr nanocomposites.

composites is calculated by ~640 $m^2 g^{-1}$, which is higher than that of pristine Gr (~290 $m^2 g^{-1}$). The increased surface area is due to the deposited Sn nanoparticles, where Sn nanoparticles could act as a spacer to prevent the restacking of Gr sheets. During the synthesis process, GO was converted to Gr, and the Sn nanoparticles were deposited on the surface of Gr simultaneously. This in situ formation process can efficiently avoid any serious stacking of Gr sheets.

To evaluate the electrochemical performance of these Sn nanoparticle decorated Gr sheets as active supercapacitor electrodes, cyclic voltammetry (CV), galvanostatic charge/discharge and electrochemical impedance spectroscopy, measurements in a three-electrode configuration were conducted. Fig. 4 (a) shows the CV curves of the Sn–Gr nanocomposites with various scan rates (10 mV s^{-1}–50 mV s^{-1}) in 2 M KNO_3 aqueous solutions. The CV

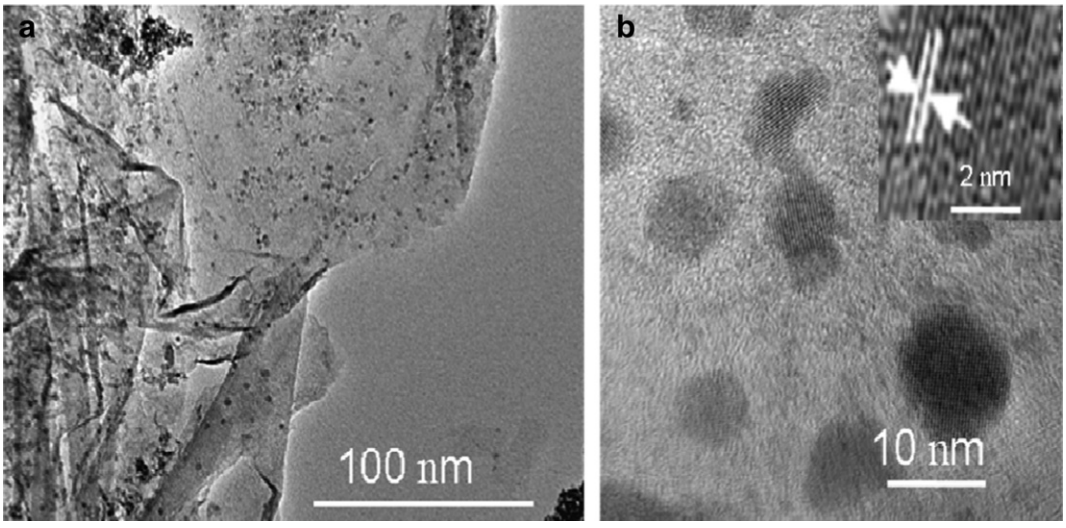

Fig. 2. (a)low-magnification and (b) HRTEM image of Sn–Gr nanocomposites, inset is the lattice image of Sn nanoparticles.

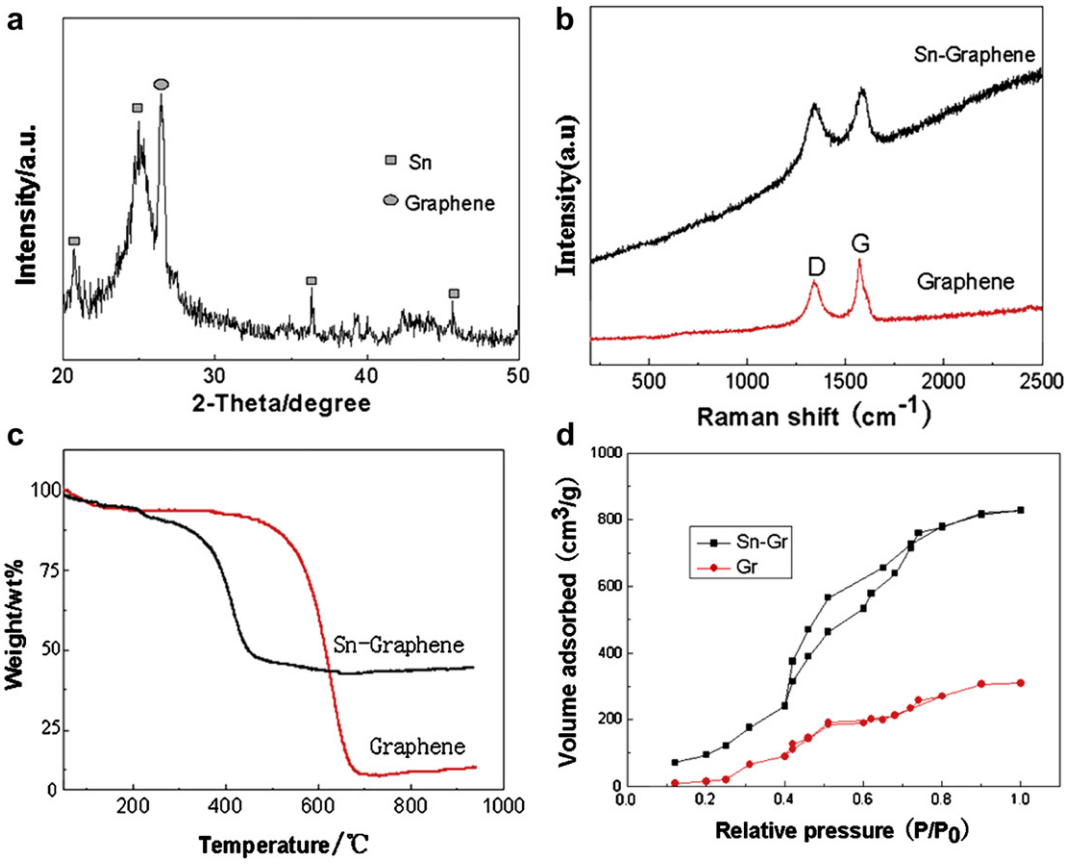

Fig. 3. (a) XRD patterns of Sn–Gr nanocomposites. (b)Raman spectra of the Sn–Gr nanocomposites, (c) TGA curves of graphene oxide and the Sn–Gr nanocomposites, the profiles were taken in air with a heating rate of 10 °C min^{-1} (d) Nitrogen adsorption–desorption isotherms of Sn–Gr nanocomposites and Gr sheets.

curves present a nearly rectangular shape at the applied scan rates, which is indicative of capacitive behavior in the regime where the current is proportional to the first power of scan rate. With the increasing of scan rate, CV curves for the composite still maintain a near rectangular shape. The specific capacitance values were calculated from the CV curves using the following equation:

$$C = \frac{\int I dt}{m\Delta V} \quad (1)$$

where I is the oxidation or reduction current, dt is time differential, m indicates the mass of the active electrode material, and ΔV indicates the voltage range of one sweep segment. The specific capacitance value calculated from the CV curve is found to be ~320 F g^{-1} at scan rate 10 mV s^{-1} in 2 M KNO_3. Although the NO_3-based electrolyte has been found to show a lower specific capacitance value, more ideal CV responses can be obtained in comparison with acidic and basic electrolytes [23,24]. This result indicates that a fast charge/discharge process exists in Sn–Gr electrode materials thus indicating a high power capability. The energy density (E) and power density (P) were derived from the CV curves using the following equations:

$$E = \frac{1}{2}C(\Delta V)^2 \quad (2)$$

$$P = \frac{E}{\Delta t} \quad (3)$$

where C is the specific capacitance of the active material, ΔV is the voltage range of one sweep segment, and Δt is the time for a sweep segment. The specific energy and specific power of the Sn–Gr electrode materials are ~36 W h kg^{-1} and 1440 W kg^{-1}, respectively.

Fig. 4 (b) exhibits galvanostatic charge and discharge curves of Sn–Gr electrodes in 2 M KNO_3 aqueous solutions at different loading current density. The electrode charge–discharge curves show a good inverse proportion at loading current density of 1.0, 2.0, 5.0 and 10.0 A g^{-1}. These curves show the nearly triangle shape even at high current density of 10.0 A g^{-1}. This is indicative of the formation of an efficient EDLC and fast ion transport. The response time of these capacitors is ~1 s, which means such supercapacitors having the fast self-discharge ability. Long cycling life is another crucial character for their practical applications [25]. The capacitance retention ratio as a function of cycle number is presented in Fig. 4c. The capacitance of Sn–Gr retained 96% of its initial capacitor after 800 cycles, which demonstrates excellent electrochemical stability. Fig. 4d shows the impedance spectra of Gr and Sn–Gr electrode material analyzed using Nyquist plots at applied potential of 0.4 V, over the frequency range between 10 kHz and 0.1 Hz. It shows a straight line in the low-frequency region and a semicircle in the high frequency region. At low frequency, the imaginary part sharply increases and a vertical line is usually observed, indicating a pure capacitive behavior [26]. The internal resistance of Sn–Gr is smaller than that of Gr, which suggests that the Sn decorated the graphene sheets materials have better conductive properties and, therefore, better electrochemical behavior. It is speculated that the low resistances of Sn–Gr composite electrode is due to its high specific surface area, which facilitates a faster cation insertion and extraction during the charge–discharge process [27].

Fig. 5 demonstrates the discharge capacity of pure graphite, Gr, and Sn–Gr over 800 cycles in the 1 M H_2SO_4 electrolyte. The

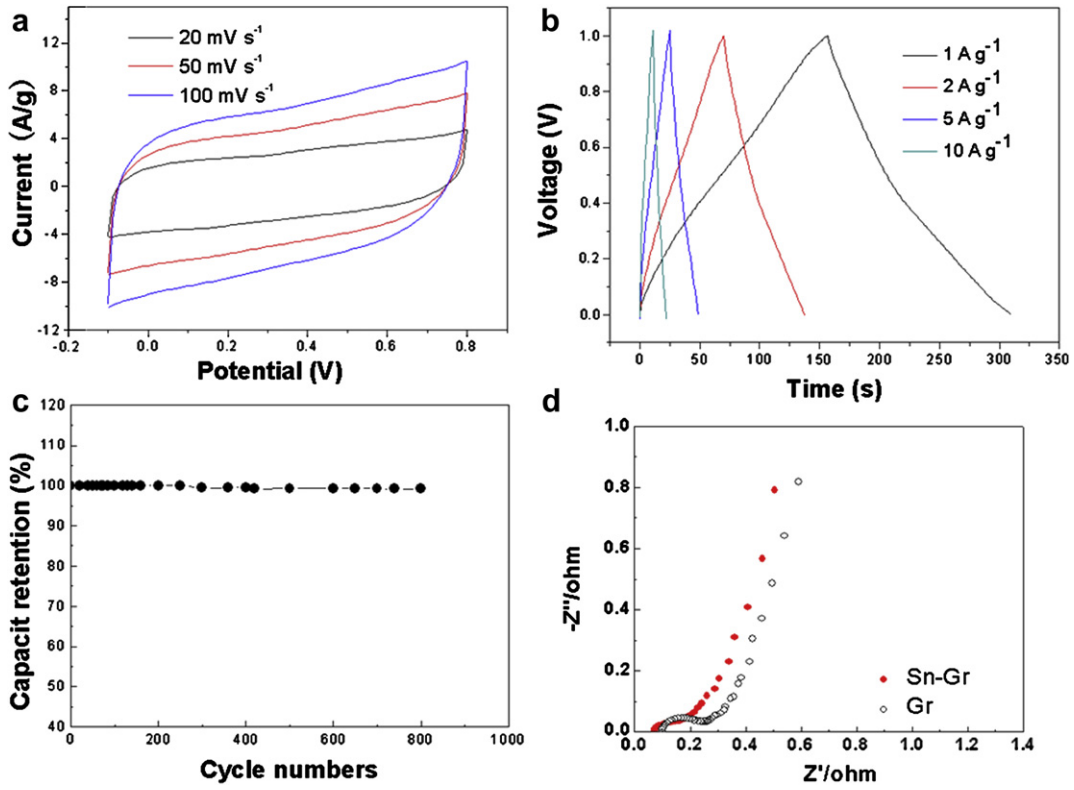

Fig. 4. (a) Cyclic voltammograms of Sn–Gr nanocomposites at different scan rates, (b) Galvanostatic charging/discharging curves measured with different current densities for the Sn–Gr nanocomposites, (c) Long-term cycling behavior of Sn–Gr nanocomposites, (d) Nyquist plot for the graphene oxide and the Sn–Gr nanocomposites at the frequency range of 0.1–10 kHz.

specific capacitance of Sn–Gr electrode is found to be 295 F g^{-1} at the 800th, which the capacitance value is higher than that of the pure Gr(120 F g^{-1}) and pure graphite (15 F g^{-1}). This can be attributed to the Sn nanoparticles uniformly dispersed over the surface of Gr, which provides reasonable rate capability during the reversible conversion reaction.

The good electrochemical properties of Sn–Gr electrode materials could be ascribed to two aspects. On the one hand, Sn nanoparticles have been intercalated into the interlayer of the Gr nanosheets, which prevents any serious stacking of the Gr nanosheets and thus increases the electrochemical accessible area. On the other hand, addition of Sn nanoparticles onto a Gr electrode could reduce the intrinsic resistance of Gr materials due to the metal active materials grown on the surface of Gr uniformly. Therefore, the electrochemical properties of Gr are corresponding improved. As a result, the as-synthesized Sn–Gr nanocomposite materials possess a good electrochemical performance, which provides an important electrode material candidate for supercapacitors.

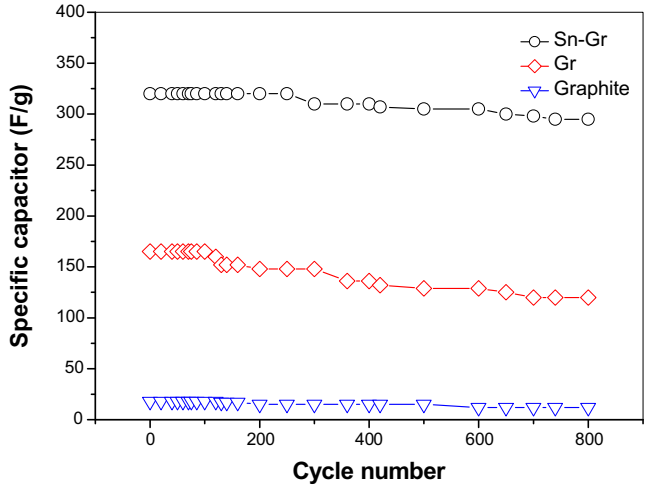

Fig. 5. Specific capacitance vs. cycle-ability of pure graphite, Gr, and Sn–Gr nanocomposites in 1 M H_2SO_4.

4. Conclusion

In summary, Sn nanoparticle decorated Gr sheets were synthesized by direct growth of Sn nanoparticles on the surface of Gr sheets during reduction of GO process. The FESEM, TEM analysis revealed the Sn nanoparticles were uniformly distributed on Gr sheet substrates. In comparison with the specific capacitance of Gr electrode, the specific capacitance of Sn–Gr nanocomposite electrode (320 F g^{-1}) is significantly improved. The high specific capacitance of the Sn–Gr electrode could be explained by the existence of Sn nanoparticles could act as a spacer to prevent the restacking of Gr sheets. The low price, abundant resources, and environmental friendliness of tin may render Sn nanoparticles decoration of graphene sheets a promising candidate for practical applications.

Acknowledgments

The authors are grateful for support from the National Natural Science Foundation of China (No.51072063), Natural Science Foundation of Henan Province (No.112300410012), Natural Science Foundation of Education Department of Henan Province (No.2011C430003), and Science Foundation of Zhengzhou City (No.20110342).

References

[1] M. Winter, R.J. Brodd, Chem. Rev. 104 (2004) 4245–4269.
[2] M.F. El-Kady, V. Strong, S. Dubin, R.B. Kaner, Science 335 (2012) 1326–1330.
[3] J.R. Miller, R.A. Outlaw, B.C. Holloway, Science 329 (2010) 1637–1639.
[4] A. Burke, Electrochim. Acta 53 (2007) 1083–1091.
[5] J.Y. Xiang, J.P. Tu, L. Zhang, Y. Zhou, X.L. Wang, S.J. Shi, J. Power Sources 195 (2010) 313–319.
[6] J. Chmiola, C. Largeot, P.-L. Taberna, P. Simon, Y. Gogotsi, Science 313 (2006) 1760–1763.
[7] N.L. Wu, Mater. Chem. Phys. 75 (2002) 6–8.
[8] T. Brezesinski, J. Wang, S.H. Tolbert, B. Dunn, Nat. Mater. 9 (2010) 146–151.
[9] A. Rudge, J. Davey, I. Raistrick, S. Gottesfeld, J.P. Ferraris, J. Power Sources 47 (1994) 89–107.
[10] M. Toupin, T. Brousse, D. Belanger, Chem. Mater. 16 (2004) 3184–3190.
[11] A. Izadi-Najafabadi, S. Yasuda, K. Kobashi, T. Yamada, D.N. Futaba, H. Hatori, M. Yumura, S. Iijima, K. Hat, Adv. Mater. 22 (2010) E235–E241.
[12] D.N. Futaba, K. Hata, T. Yamada, T. Hiraoka, Y. Hayamizu, Y. Kakudate, O. Tanaike, H. Hatori, M. Yumura, S. Iijima, Nat. Mater. 5 (2006) 987–994.
[13] Y. Zhu, S. Murali, W. Cai, X. Li, J.W. Suk, J.R. Potts, R.S. Ruoff, Adv. Mater. 22 (2010) 3906–3924.
[14] M. Segal, Nat. Nanotechnol. 4 (2009) 612–614.
[15] M.D. Stoller, S.J. Park, Y.W. Zhu, J.H. An, R.S. Ruoff, Nano Lett. 8 (2008) 3498–3502.
[16] Y. Wang, Z.Q. Shi, Y. Huang, Y.F. Ma, C.Y. Wang, M.M. Chen, Y.S. Chen, J. Phys. Chem. C 113 (2009) 13103–13107.
[17] W. Lv, D.M. Tang, Y.B. He, C.H. You, Z.Q. Shi, X.C. Chen, C.M. Chen, P.X. Hou, C. Liu, Q.-H. Yang, ACS Nano 3 (2009) 3730–3736.
[18] K.H. Chang, Y.F. Lee, C.C. Hu, C.I. Chang, C.L. Liu, Y.L. Yang, Chem. Commun. 46 (2010) 7957–7959.
[19] S.Y. Yang, K.H. Chang, H.W. Tien, Y.F. Lee, S.M. Li, Y.S. Wang, J.Y. Wang, C.C.M. Ma, C.C. Hu, J. Mater. Chem. 21 (2011) 2374–2380.
[20] Y. Zhu, M.D. Stoller, W. Cai, A. Velamakanni, R.D. Piner, D. Chen, R.S. Ruoff, ACS Nano 4 (2010) 1227–1233.
[21] S.R.C. Vivekchand, C.S. Rout, K.S. Subrahmanyam, A. Govindaraj, C.N.R. Rao, J. Chem. Sci. 120 (2008) 9–13.
[22] Y.W. Zhu, S. Murali, M.D. Stoller, A. Velamakanni, R.D. Piner, R.S. Ruoff, Carbon 48 (2010) 2118–2122.
[23] C.C. Hu, C.C. Wang, F.C. Wu, R.L. Tseng, Electrochim. Acta 52 (2007) 2498–2505.
[24] H.A. Andreas, B.E. Conway, Electrochim. Acta 51 (2006) 6510.
[25] S.Y. Yang, K.H. Chang, H.W. Tien, Y.F. Lee, S.M. Li, Y.S. Wang, et al., J. Mater. Chem. 21 (2011) 2374–2378.
[26] W. Xiong, M.X. Liu, L.H. Gan, Y.K. Lv, Y. Li, L. Yang, et al., J. Power Sources 196 (2011) 10461–10464.
[27] K. Zhang, L.L. Zhang, X.S. Zhao, J. Wu, Chem. Mater. 22 (2010) 1392–1401.